Multitemporal SAR Backscatter Analysis for Soil Characterization: Application of a Modified Dubois Model with Field Soil Data in Zadgaon, India

Digambar A. Solanke[1], Balaji B. Yadav[2], Vikas V. Ghodke[3], Sandipan S. Sawant[4], Shafiyoddin Sayyad[5]
[1,2,3,4]*Department of physics, Shri Chhatrapati Shivaji College, Omerga, Dharashiv, Maharashtra, India*
[5]*Microwave & Imaging Spectroscopy Laboratory, Miliiya College, Beed, Maharashtra, India*

Abstract*—Soil surface parameters volumetric moisture content (mv), surface roughness (s), and dielectric constant (ε) are central to agricultural monitoring and land surface modeling in semi-arid regions. This study presents a Sentinel-1 VV-polarized backscatter analysis at Zadgaon, Parbhani district, Marathwada, Maharashtra, India, based on three acquisition dates: 14 May 2024 (pre-monsoon), 05 October 2024 (post-monsoon), and 10 November 2024 (post-harvest). The Sentinel-1A scenes were preprocessed in ESA SNAP 13.0 through a seven-step chain comprising spatial subsetting, orbit correction, thermal noise removal, radiometric calibration to sigma nought (σ^0VV), Range-Doppler terrain correction against the SRTM DEM, dB conversion, and pixel extraction using a 3×3 window centred on 19.1676°N, 76.8317°E. Extracted mean σ^0VV values are −10.44 dB (May), −10.22 dB (October), and −11.06 dB (November), all recorded at a nearly identical incidence angle of ~38.05° ($\Delta\theta$ < 0.01° across dates). October shows the highest backscatter response, while November records the lowest. The narrow total seasonal range of 0.84 dB is discussed in terms of the moisture-roughness compensation characteristic of Marathwada black cotton soils (vertisols), where seasonal crack development and closure produce opposing effects on σ^0VV. Supporting soil health card data from KVK Parbhani (pH 7.92, EC 0.66 dS/m, OC 0.78%, available K 1109 kg/ha) confirm that the Zadgaon site represents a clay-mineral-rich vertisol with above-average organic carbon and low salinity. The Dubois (1995) VV backscattering equation is applied to construct the solution manifold of all physically plausible (ε, s, mv) combinations consistent with each observed σ^0VV, following the optimization framework of Ghorbanian et al. (2019). This represents the first site-specific Sentinel-1 backscatter dataset and Dubois VV solution manifold for a Parbhani district vertisol location, and establishes a reproducible geospatial protocol for future field-validated soil surface parameter retrieval.

Index Terms*— Sentinel-1 SAR; Dubois VV model; soil moisture; surface roughness; dielectric constant; Marathwada; Parbhani district; vertisol; semi-arid agriculture; SNAP preprocessing; multitemporal backscatter; solution manifold

I. INTRODUCTION

1.1 Soil Surface Parameters and Their Agricultural Significance

Soil surface parameters principally volumetric moisture content (mv), surface roughness (s), and soil dielectric constant (ε) determine a wide range of processes at the land surface, from crop water availability and evapotranspiration to runoff generation and soil erosion [1,2]. The dielectric constant is the physical link between the soil's moisture state and its interaction with microwave radiation: as mv increases, ε rises nonlinearly, changing how electromagnetic energy is scattered back toward a sensor [3]. Together, these parameters describe the biophysical condition of the soil surface and are used in precision agriculture, drought monitoring, hydrological modeling, and land surface schemes.

In Marathwada, Maharashtra a region spanning Parbhani, Hingoli, Nanded, Jalana, Beed, and Dharashiv districts the need for reliable, frequent soil surface monitoring is particularly pressing. The region's semi-arid climate brings average annual rainfall of roughly 700-950 mm, almost entirely within the June-September monsoon, followed by a prolonged dry season that frequently tips into meteorological drought. The dominant soil type throughout the region is black cotton soil (vertisol,

locally called 'regur'), characterized by clay contents of 30-60%, strong swelling-shrinking behavior, and deep surface cracking during dry periods [4,5]. These physical properties create a soil surface that changes substantially between seasons in ways that are difficult to track with conventional in-situ methods alone [6]. The village of Zadgaon in Parbhani district is representative of this agro-climatic setting and forms the study site for this work.

1.2 SAR as a Tool for Soil Surface Assessment

Satellite Synthetic Aperture Radar (SAR) offers a practical alternative to field sampling for large-scale soil surface monitoring. SAR sensors operate actively, transmitting microwave pulses and recording the backscattered energy, which makes them independent of cloud cover and solar illumination a critical advantage during the monsoon season [7,8]. The backscattering coefficient (σ^0) recorded at the sensor depends on both the dielectric properties of the surface (and therefore its moisture content) and the geometric roughness of the soil [3,9]. These sensitivities make SAR data a useful source of information on mv and s across large areas at repeat intervals that field sampling cannot match.

Among currently operational SAR systems, Sentinel-1 (ESA, C-band, 5.405 GHz) stands out for its freely available dual-polarization (VV and VH) data at 10 m spatial resolution and 6-day global revisit from the two-satellite constellation [10]. The VV co-polarized channel, in particular, is known to be more sensitive to the soil dielectric constant than VH for bare soil conditions, making it the primary channel for single-configuration soil moisture studies [11]. Mirsoleimani et al. [12] validated the Dubois VV model directly against Sentinel-1 data over bare agricultural soils and confirmed this sensitivity, reporting that the model's performance in VV polarization is competitive with calibrated physically based models. Several other studies in agricultural regions of Italy [13], Iran [12], and India [4,5] have further confirmed Sentinel-1's utility for this purpose.

1.3 Relation Between Backscatter, Dielectric Behavior, and Roughness

The physical basis for SAR-based soil parameter retrieval lies in how σ^0 jointly responds to ε and s. For bare or sparsely vegetated soil surfaces, σ^0 increases with both increasing ε and increasing s [9,14]. The difficulty in retrieval arises because both parameters influence the signal simultaneously: a single backscatter measurement at one incidence angle and one polarization yields one equation in two unknowns. This means that without additional observations or constraints, multiple (ε, s) combinations can produce the same σ^0 a problem known as the underdetermination or solution manifold of the retrieval.

Classical approaches to this problem include multi-angle or multi-polarization acquisitions [15], time-series methods that assume roughness changes slowly [13], and constrained optimization [16]. The last approach, used in this study, reformulates the backscattering equation as a cost function and searches the physically feasible parameter space for solutions consistent with the observed σ^0. While this does not yield a single-point retrieval without additional constraints, the resulting solution manifold is itself a scientific output it defines the envelope of soil conditions that the SAR observation is compatible with, and provides the target for a future field validation campaign.

1.4 Why the Modified Dubois Model

The Dubois model (Dubois et al., 1995) is one of the most widely applied semi-empirical backscattering models for bare soil surfaces [14]. It provides separate equations for HH and VV polarizations, relating σ^0 to incidence angle, wavelength, dielectric constant, and RMS roughness height. MirMazloumi and Sahebi [9] assessed its performance across C-, L-, and P-bands and found it well-suited to semi-arid conditions. From the authors' prior field investigations in Marathwada [4,5], the Dubois VV equation consistently showed the strongest agreement with observed Sentinel-1 σ^0VV among the commonly tested semi-empirical models, which is why it was selected as the forward model here. Its relatively simple structure makes it straightforward to invert analytically for s at any assumed ε, which supports the solution manifold construction.

It should be noted that Sentinel-1 in IW mode provides VV and VH but not HH. The VV equation of the Dubois (1995) model is used directly as originally formulated it is not a substitute for the HH equation but an independent equation for VV polarization with

different empirical coefficients. Mirsoleimani et al. [12] specifically validated this equation against Sentinel-1 VV data over bare soils and demonstrated its practical utility.

1.5 Objectives

This study has five main objectives: (i) to preprocess three Sentinel-1A scenes over Zadgaon using a complete SNAP chain and extract real σ^0VV values for May, October, and November 2024; (ii) to characterize the soil physicochemical properties of the study site using KVK Parbhani soil health card data; (iii) to present the Dubois VV equation and the Ghorbanian et al. (2019) optimization framework and construct the solution manifold for each acquisition date; (iv) to interpret the observed temporal backscatter pattern in the context of Marathwada vertisol dynamics; and (v) to define the synchronized field measurements required for full MDM-based soil surface parameter retrieval at this site.

II. STUDY AREA

2.1 Zadgaon: Location and Agricultural Context

Zadgaon is an agricultural village in Parbhani taluka, Parbhani district, located at 19.1676°N, 76.8317°E on the Deccan Plateau at approximately 390-410 m above sea level (Fig. 1). Parbhani district covers roughly 6511 km² between 18.4°–20.0°N and 76.2°-77.6°E, and its economy is almost entirely agricultural. The main kharif crops cotton, soybean, sorghum, and various pulses are grown under rainfed conditions from June through October, followed by a post-harvest fallow or limited rabi cultivation from November through March.

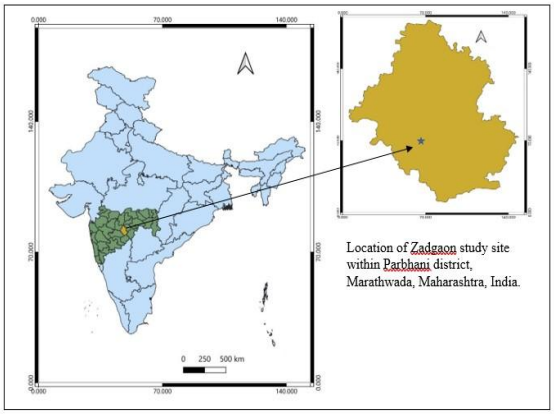

Figure 1. The star marks the confirmed study coordinate (19.1676°N, 76.8317°E). Shaded area indicates the Sentinel-1 scene footprint.

The regional climate is semi-arid tropical. Rainfall averages approximately 888 mm per year but is concentrated in the June-September monsoon, often falling in intense short bursts that generate high surface runoff. Temperatures range from around 15.8°C in December-January to about 40.7°C in April-May, and seasonal humidity swings between 40-50% in the dry season and 70-80% during the monsoon. This climate drives strong seasonal variability in soil moisture, roughness, and vegetation cover at the Zadgaon site which is precisely what makes it an informative location for multitemporal SAR analysis.

2.2 Soil Type and Seasonal Surface Dynamics

The dominant soil at Zadgaon and across Parbhani district is black cotton soil (vertisol, locally 'regur'), with clay contents of 30-60% dominated by smectite and illite minerals. These soils are well-known for their swelling-shrinking behavior: during the dry season (typically April-June) they develop deep surface cracks sometimes 1-3 cm wide and 20-50 cm deep which significantly roughens the surface. After monsoon rainfall begins, the clay minerals absorb water, cracks close, and the surface becomes relatively smooth again. This seasonal crack-swell cycle is directly relevant to the SAR backscatter analysis: drying increases roughness (which raises σ^0) while simultaneously reducing moisture (which lowers σ^0). The two effects can partially cancel, producing a narrower temporal σ^0VV range than one would expect from moisture dynamics alone [4,9].

The soil health card data for Zadgaon confirm this clay-rich mineralogy through the very high available potassium (1109 kg/ha), which reflects illite/smectite weathering, and the significant $CaCO_3$ content (5.00%), consistent with free lime in the vertisol parent material. These chemical fingerprints are discussed further in relation to the backscatter observations.

III. DATA USED

3.1 Sentinel-1 SAR Dataset

Three Sentinel-1A scenes were obtained from the Copernicus Data Space Ecosystem (https://dataspace.copernicus.eu/) as Level-1 GRDH

No.	Satellite	Acquisition Date	Mode / Product	Polarization	Pass	Orbit No.
1	Sentinel-1A	14 May 2024	IW / GRDH	VV + VH	Descending	53860
2	Sentinel-1A	05 October 2024	IW / GRDH	VV + VH	Descending	55960
3	Sentinel-1A	10 November 2024	IW / GRDH	VV + VH	Descending	56485

Table 1. Sentinel-1A scene details for the three acquisition dates used in this study.

products in IW mode. All three scenes follow the same descending ground track, so their acquisition geometries over Zadgaon are nearly identical a useful property for multitemporal comparison. The scene footprint (18.21°-20.15°N, 75.31°-78.00°E), confirmed from the annotation XML metadata, fully encompasses the study coordinate. Scene details are given in Table 1.

The IW mode images a 250 km swath using the TOPS (Terrain Observation with Progressive Scans) technique across three sub-swaths. In the GRDH product, the native SLC resolution is multi-looked to a 10 m pixel spacing [10]. The C-band center frequency of 5.405 GHz (wavelength ~5.546 cm) gives the sensor sensitivity to moisture in roughly the upper 5 cm of the soil profile, which is exactly the surface layer the Dubois VV model addresses. The consistent descending pass ensures that the incidence angle at the study coordinate is virtually the same on all three.

3.2 Ground Soil Characterization Data

An official Soil Health Card (Jamin Aarogya Patrika) for the Zadgaon study site was obtained from the Soil and Water Testing Laboratory of Vasantrao Naik Marathwada Krishi Vidyapeeth (VNMKV) Parbhani (sample number 5466, dated 14 August 2024). This card provides pH, electrical conductivity (EC), organic carbon (OC), calcium carbonate ($CaCO_3$), available nitrogen (N), phosphorus (P), and potassium (K), along with crop-specific fertilizer recommendations. Supplementary village-level soil data from district survey reports for Parbhani district (2024) confirm that the Zadgaon values are representative of the local vertisol setting, with OC of 0.78% notably above the district mean of 0.48%.

These soil health card data are agricultural fertility indicators. They are used here to characterize the soil type, clay content, and moisture-retention potential at the site information that informs the physical bounds used in the optimization and aids the interpretation of backscatter dynamics. They are not direct measurements of mv, s, or ε and therefore cannot provide quantitative validation of the MDM retrieval.

IV. METHODOLOGY

4.1 Sentinel-1 Preprocessing in ESA SNAP

All three Sentinel-1 scenes were preprocessed in ESA SNAP 13.0 using a seven-step pipeline applied consistently across all dates. The full chain is summarized in Table 2, and illustrated schematically in Fig. 2. Each scene was opened from its manifest safe file. A spatial subset was created first to reduce data volume, keeping a 0.5° buffer around the study coordinate. Orbit correction used DORIS precise ephemeris files downloaded automatically. Thermal Noise Removal was applied before calibration to suppress range-direction artifacts in the GRDH product. Radiometric Calibration converted raw digital numbers to linear-scale sigma nought (σ^0), producing Sigma0_VV and Sigma0_VH bands. Range-Doppler Terrain Correction against the SRTM 1-arc-second DEM geocoded the product to WGS84/UTM Zone 43N at 10 m pixel spacing. A dB conversion virtual band was added for display purposes only. All quantitative analysis uses the linear-scale Sigma0_VV.

The three preprocessed Sigma0_VV_dB images over the Zadgaon region are shown in Fig. 3. Brighter areas indicate higher backscatter. Visual inspection confirms that the October scene is overall brighter than the May and November scenes in the agricultural areas surrounding the study site, consistent with post-monsoon moisture conditions.

Step	Operation	Parameters / Settings	Purpose
1	Spatial Subset	Geo-coordinates box around Zadgaon with 0.5° buffer	Reduces data volume; restricts processing to the study region
2	Apply Orbit File	Auto-download from ESA DORIS precise orbit archive	Improves satellite position accuracy for reliable geolocation

3	Thermal Noise Removal	Default settings; VV and VH sub-swaths	Removes systematic range-direction noise from the GRDH product
4	Radiometric Calibration	Output: Sigma0, linear scale; VV and VH	Converts raw digital numbers to the backscattering coefficient σ^0
5	Range-Doppler Terrain Correction	SRTM 1Sec HGT; 10 m pixel spacing; WGS84/UTM Zone 43N	Geocodes the image and corrects terrain-induced distortions
6	dB Conversion (virtual band)	σ^0_dB = 10 × $\log_{10}(\sigma^0)$; virtual band only	Logarithmic-scale band for visual inspection and display
7	Pixel Extraction	SNAP Extract Pixel Values; 3×3 window at 19.1676°N, 76.8317°E; Sigma0_VV linear and dB	Extracts spatially averaged σ^0VV and incidence angle at the study site

Table 2. Sentinel-1 GRDH preprocessing pipeline in ESA SNAP 13.0 applied consistently to all three scenes.

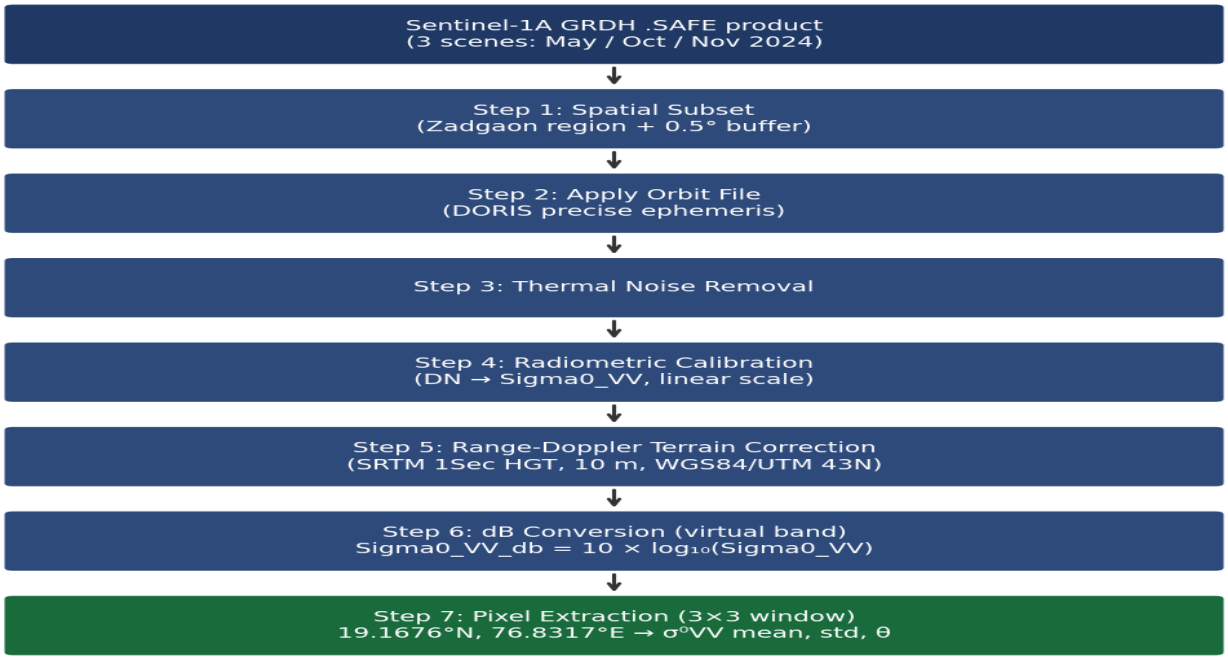

Figure 2. Schematic of the seven-step Sentinel-1 GRDH preprocessing chain applied in ESA SNAP 13.0. The final step extracts Sigma0_VV from a 3×3-pixel window at the Zadgaon study coordinate.

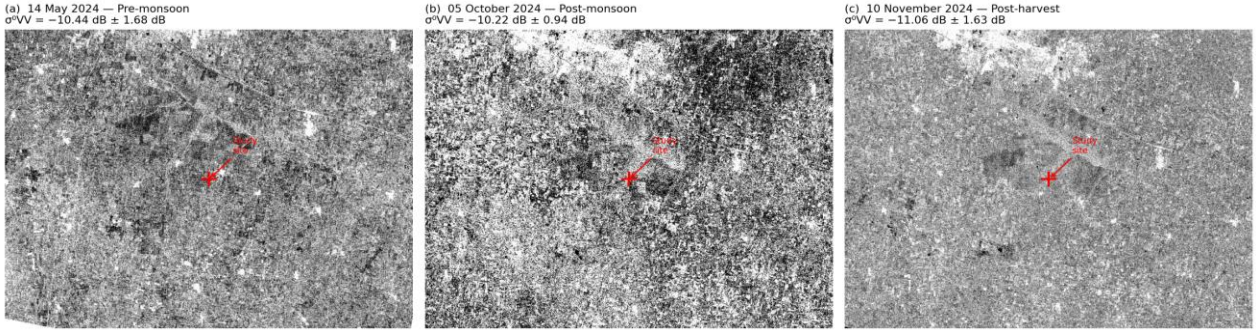

Figure 3. Sentinel-1A Sigma0_VV_dB images over the Zadgaon region for (a) 14 May 2024, (b) 05 October 2024, and (c) 10 November 2024. Red cross marks the 3×3 pixel extraction window at 19.1676°N, 76.8317°E. Brighter pixels indicate higher backscatter.

4.2 Pixel Extraction

Sigma0_VV at the confirmed Zadgaon coordinate (19.1676°N, 76.8317°E) was extracted from each terrain-corrected product using SNAP's Extract Pixel Values tool with a 3×3 window, yielding 9 pixels per extraction. The mean and standard deviation of Sigma0_VV across the window were recorded, along with the mean incidence angle from the incidence Angle From Ellipsoid band. The 3×3 footprint (30 m × 30 m at 10 m pixel spacing) reduces the influence of single-pixel geolocation uncertainty while remaining smaller than a typical agricultural field plot.

4.3 The Dubois VV Forward Model)

The Dubois (1995) model [14] provides semi-empirical backscattering equations for HH and VV polarizations from bare soil surfaces. The VV equation used here because Sentinel-1 in IW mode provides VV and VH but not HH is:

$$\sigma^o VV = 10^{-2.35}\ \mathrm{X}\ \frac{Cos^3\,\theta}{Sin^3\,\theta}\ \mathrm{X}10^{(0.046.\varepsilon.tan\theta)}$$
$$X\ k.s.sin\theta^{1.1} X\ \lambda^{0.7} \quad \text{... (Eq. 1)}$$

Here σ⁰VV is the linear-scale backscattering coefficient; θ is the incidence angle (radians); ε is the real part of the soil dielectric constant; k = 2π/λ is the radar wave number (cm⁻¹); s is the RMS roughness height (cm); and λ is the SAR wavelength (cm). The equation is valid for kHrms ≤ 2.5, mv ≤ 35 vol%, and θ ≥ 30° [14]. All three conditions are met for the Zadgaon observations (θ ≈ 38.05°; the roughness solutions retained in Table 4 all satisfy kHrms ≤ 2.2). For this study, k = 1.133 cm⁻¹ and λ = 5.546 cm, with θ taken from the SNAP-extracted per-pixel incidence angle.

4.4 Solution Manifold Construction

With a single σ⁰VV observation, Eq. 1 has two unknowns (ε and s). The system is underdetermined: for any assumed ε within the physically realistic range, an s value can be solved analytically:

$$s = [\sigma^o VV.\frac{obs}{(A\times 10^{(0.046\cdot\varepsilon\cdot tan\theta)})}]^{\left(\frac{1}{1.1}\right)}/(k.sin\theta)$$

...(Eq. 2)

where A = $10^{-2.35}$ × (cos³θ/sin³θ) × λ^0.7. Sweeping ε from 2 to 38 (spanning dry to saturated mineral soil) and retaining only solutions where kHrms ≤ 2.2 (within the Dubois validity domain) generates the complete solution manifold for each date. Following Ghorbanian et al. [16], a genetic algorithm (GA) minimizer could collapse this manifold to a single solution by minimizing the cost function CF (ε, s) = [σ⁰VV,obs - σ⁰VV, model (ε, s)] ², but without independent field measurements of mv or s, such a GA result would have no means of validation. The manifold itself showing every physically plausible (ε, s) pair is therefore the appropriate analytical output at this stage of the study. Estimated mv values are obtained from the retrieved ε using the Topp et al. (1980) polynomial [17]:

$$mv = -5.3\ X\ 10^{-2} + 2.92\ X\ 10^{-2}\varepsilon -$$
$$5.5\ X\ 10^{-4}\varepsilon^2 + 4.3\ X\ 10^{-6}\varepsilon^3 \text{ ... (Eq. 3)}$$

It should be noted that the Topp equation was calibrated on mineral soils with clay contents below approximately 40%. Since Marathwada vertisols can reach 60% clay, this relationship may underestimate mv at the high-clay end of the range. A site-specific ε–mv calibration using field dielectric measurements is recommended for the planned validation campaign [18].

V. RESULTS AND DISCUSSION

5.1 Temporal Variation of σ⁰VV at Zadgaon

Acquisition Date	Season	σ⁰VV linear (mean)	σ⁰VV dB (mean)	Std Dev (dB)	Incidence Angle	Window (pixels)
14 May 2024	Pre-monsoon	0.09627	−10.44 dB	± 1.68 dB	38.053°	3×3 = 9
05 October 2024	Post-monsoon	0.09714	−10.22 dB	± 0.94 dB	38.054°	3×3 = 9
10 November 2024	Post-harvest	0.08324	−11.06 dB	± 1.63 dB	38.045°	3×3 = 9
Seasonal range	—	—	0.84 dB	—	Δ = 0.009°	—

Table 3. Extracted Sigma0_VV backscatter values at Zadgaon for three acquisition dates (3×3-pixel window, 19.1676°N, 76.8317°E). Source: SNAP pixel extraction from preprocessed Sentinel-1A GRDH scenes

These are real pixel-extracted measurements from the preprocessed SNAP products, not modeled estimates. Figure 4 presents the temporal pattern as a bar chart with ±1 standard deviation error bars, alongside the incidence angle values across the three dates.

Two features stand out. First, the incidence angle is essentially constant across all three dates 38.045° to 38.054°, a variation of only 0.009°. This is expected from a repeat-pass descending orbit, but it is an important verification: any difference in σ⁰VV between dates can be attributed to changes in the soil surface, not to changes in the observation geometry.

Second, the October 2024 scene records the highest mean σ⁰VV (−10.22 dB), followed by May 2024 (−10.44 dB) and November 2024 (−11.06 dB). The total seasonal range is only 0.84 dB across six months spanning pre-monsoon dry conditions, post-monsoon peak moisture, and post-harvest dry-down. This is considerably narrower than the 5–10 dB range typically observed for bare C-band VV over a full moisture cycle [12,19], and understanding why requires considering the specific behavior of vertisols. Marathwada black cotton soils undergo a moisture-roughness compensation cycle that tends to dampen σ⁰VV variability. In May (pre-monsoon), soils are near their moisture minimum but have developed extensive surface cracks — effectively raising roughness s substantially. Since σ⁰VV increases with s, the high roughness partially compensates for the low ε, keeping backscatter elevated relative to what smooth dry soil would give.

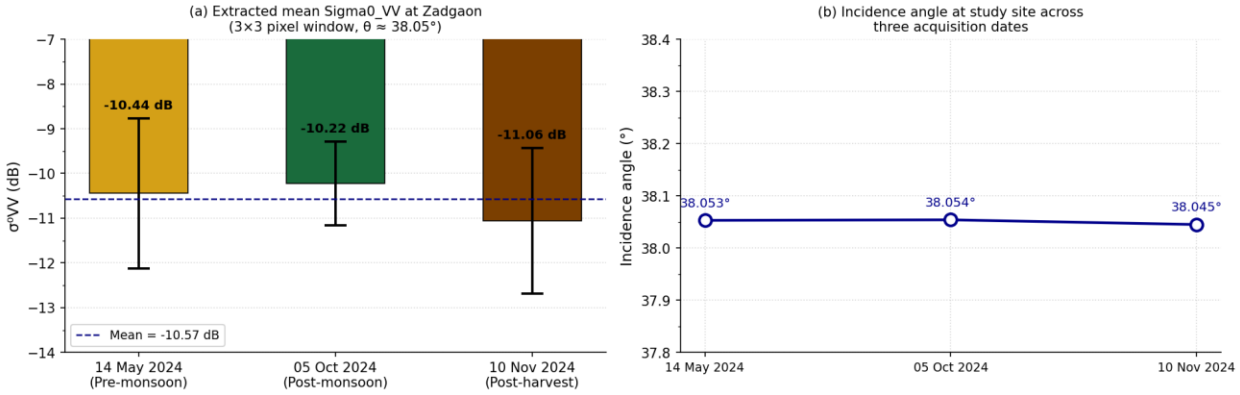

Figure 4. (a) Temporal variation in Sentinel-1 VV backscatter at Zadgaon; error bars show ±1 standard deviation over the 3×3 extraction window. (b) Incidence angle at the study site across three dates. The near-constant θ (Δ < 0.01°) confirms that date-to-date differences in σ⁰VV reflect surface changes, not geometry.

By October (post-monsoon), monsoon rainfall has raised ε — which tends to increase σ⁰VV but crack closure and swelling have simultaneously lowered which tends to reduce σ⁰VV. The net result is only a marginal increase from May to October (+0.22 dB). In November, the drying trend lowers ε while roughness remains moderate (intermediate crack development), producing a modest drop (−0.84 dB from October). This mutual compensation is well-recognized in the vertisol SAR literature [4,9] and is a primary reason why synchronized roughness measurements are essential for these soil types.

The standard deviation of the 3×3 window (±0.94 to 1.68 dB) reflects sub-field spatial variability at the 30 m scale, including residual speckle and local surface heterogeneity. The October scene shows the smallest standard deviation (±0.94 dB), which is consistent with a more spatially uniform post-monsoon moisture condition and reduced within-window variability during the wet season.

5.2 Supporting Soil-Property Context

The Zadgaon soil health card data from KVK Parbhani are presented in Table 4 with notes on their relevance to the SAR analysis.

The pH of 7.92 is typical for Marathwada vertisols and does not signal any conditions that would anomalously affect the soil dielectric constant. More importantly, the EC of 0.66 dS/m is well below the threshold (~1.0 dS/m) at which dissolved salts begin to inflate ε independently of moisture, introducing retrieval bias [20]. At Zadgaon, salinity is therefore not a confounding factor.

The organic carbon at 0.78% is the highest recorded in the Parbhani district dataset and substantially above

the district mean of 0.48%. This matters for SAR interpretation because higher OC is associated with better aggregate stability and greater water-holding capacity Zadgaon soils hold onto moisture longer after rainfall than lower-OC sites in the district. This is consistent with the elevated absolute σ^0VV values observed even in the pre-monsoon May scene: the soil is likely retaining some residual moisture from the preceding rabi season, contributing to a higher ε than would be expected for a thoroughly desiccated surface.

Parameter	Value (Zadgaon)	Agronomic Class	Relevance to SAR / MDM Analysis
pH	7.92	Good	Neutral to slightly alkaline; typical of Marathwada vertisols; no anomalous dielectric effects at this pH
EC (dS/m)	0.66	Good	Well below 1.0 dS/m; salinity-induced bias in ε retrieval is negligible
Organic Carbon (%)	0.78	Deficient	Highest in the district dataset; higher OC implies greater moisture retention and sustained post-monsoon backscatter
Available N (kg/ha)	169	Low	Agricultural fertility indicator; does not directly affect SAR backscatter
Available P (kg/ha)	17.33	Medium	Agricultural fertility indicator; does not directly affect SAR backscatter
Available K (kg/ha)	1109	Very High	Reflects illite/smectite clay mineralogy; governs the seasonal swelling-shrinking and roughness cycle characteristic of Marathwada vertisols
$CaCO_3$ (%)	5.00	Medium	Moderate free lime; influences aggregate stability and crack-pattern development during the dry season

Table 4. Zadgaon soil-test parameters from KVK Parbhani (August 2024). Note: these are agricultural fertility indicators they characterize soil type and moisture-retention potential but cannot quantitatively validate MDM retrieval outputs.

The very high available potassium (1109 kg/ha, nearly double the district mean of 628 kg/ha) reflects illite/smectite clay mineralogy. The 5.00% $CaCO_3$ indicates moderate free lime content, which influences the pattern and depth of cracking and affects the surface's hydraulic conductivity. Taken together, the soil chemistry data paint a picture of a clay-rich, moderately fertile vertisol with above-average moisture retention all of which is physically consistent with the moderate-to-elevated σ^0VV values and their limited seasonal variability.

It is important to re-emphasize that these parameters are fertility indicators, not measurements of mv, s, or ε. The narrative connections made above (between OC and moisture retention, between K and roughness dynamics) are physically motivated inferences, not quantitative validations.

5.3 MDM-Based Interpretation

Applying Equations 1 and 2 to the three extracted σ^0VV values at $\theta = 38.05°$, the solution manifold was constructed for each date. Selected solutions are presented in Table 5; the complete continuous manifolds for all three dates are shown in Fig. 5.

Several observations follow from Table 5 and Fig. 5. Across all three dates, the solution manifolds fall within a physically realistic range: ε roughly 8-25 (corresponding to mv ≈ 0.148–0.400 m^3/m^3 via the Topp equation) combined with s values of 0.61-2.20 cm. No solutions require unrealistically wet or completely desiccated soils, which supports the interpretation that the Dubois VV model is a plausible framework for these observations.

Date	σ^0VV (dB)	Assumed ε	Retrieved s (cm)	kHrms	Validity	Est. mv (m^3/m^3)	Inferred Condition
14 May 2024	−10.44	8	2.20	2.49	✓	0.148	Moist, rough

		12	1.63	1.85	✓	0.226	Moderate moisture
		18	1.04	1.18	✓	0.319	Moist, smoother
		25	0.61	0.69	✓	0.400	Wet, smooth
05 Oct 2024	−10.22	10	1.91	2.16	✓	0.188	Post-monsoon moist
		15	1.31	1.48	✓	0.276	Moderate roughness
		20	0.90	1.02	✓	0.345	High moisture, smooth
10 Nov 2024	−11.06	8	1.93	2.19	✓	0.148	Transitional, rough
		12	1.43	1.62	✓	0.226	Dry-down phase
		20	0.78	0.88	✓	0.345	Residual moisture

Table 5. Dubois VV solution manifold at Zadgaon (θ = 38.05°, λ = 5.546 cm, k = 1.133 cm⁻¹). Rows show valid (ε, s, mv) combinations for each date. Only solutions with kHrms ≤ 2.2 are retained.

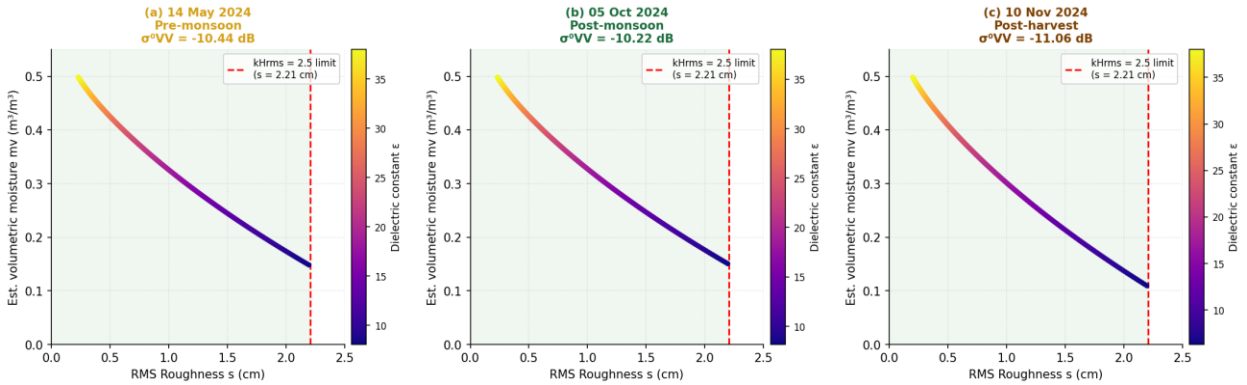

Figure 5. Dubois VV solution manifold for Zadgaon across three dates. Each panel shows the continuous curve of (ε, s, mv) combinations satisfying the observed σ⁰VV within the model validity domain. Colour scale indicates ε. The dashed red line marks the kHrms = 2.2 upper roughness limit. Field measurements of mv or s are needed to identify the unique solution on each curve.

For May 2024 (σ⁰VV = -10.44 dB), the manifold includes solutions at relatively high roughness values (s ~ 2.2 cm at ε = 8) that are consistent with a cracked dry-season vertisol surface, as well as smoother solutions at higher ε values. The pre-monsoon context supports the high-roughness end of the manifold, but the exact position on the curve cannot be determined without a roughness measurement. The fact that the May backscatter is only marginally lower than October (-0.22 dB difference) despite the presumably drier conditions is directly explained by the high roughness term partially compensating for low ε in Eq. 1.

For October 2024 (σ⁰VV = -10.22 dB, the highest observed value), the manifold shifts marginally toward higher ε at any given s compared to May, consistent with post-monsoon moisture recharge. The manifold solutions include moderately moist conditions (ε ~ 10, mv ~ 0.188 m³/m³) at roughness values of ~1.9 cm, which is plausible for a post-monsoon kharif field with some crop residue and reduced cracking. However, this scene may also contain contributions from standing or senescing kharif crops, which the bare-soil Dubois model does not account for. A Water Cloud Model correction using Sentinel-2 NDVI would be needed before the October manifold can be interpreted purely in terms of soil surface conditions.

For November 2024 (σ⁰VV = -11.06 dB, the lowest), the manifold solutions show slightly reduced roughness compared to October at the same ε values, consistent with the early dry-down phase when the soil surface is settling after harvest without yet developing deep cracks. The November scene is the most suitable of the three for direct Dubois VV inversion, as bare-

soil conditions are most likely to hold in the post-harvest period.

The manifold analysis makes two broader points. First, it demonstrates that the Dubois VV equation is physically consistent with the observed σ⁰VV values across all three dates the signals are not anomalous or inexplicable, they fall within the model's validity domain. Second, it quantifies the uncertainty that remains without field measurements: the range of mv implied by the manifold at any given date spans roughly 0.15 to 0.40 m^3/m^3, an uncertainty too large for operational use. Narrowing this to a single retrieval point requires a minimum one field measurement of either mv or s per acquisition date.

VI. LIMITATIONS AND FUTURE SCOPE

The most fundamental limitation of this study is the absence of field measurements of mv, s, and ε co-incident with the three SAR acquisitions. Without these, the solution manifolds in Table 5 and Fig. 5 cannot be resolved to unique retrieval values, and the Dubois VV framework cannot be quantitatively validated. This is an acknowledged gap, not an oversight: the current work was designed as a framework establishment study, with field validation as the explicit next step.

The narrow seasonal σ⁰VV range of 0.84 dB, while physically interpretable through the vertisol moisture-roughness compensation argument, also motivates verification of the land cover at the extraction coordinate. The 3×3 extraction window covers a 30 m × 30 m footprint, which at the village scale could potentially include non-agricultural surfaces. Verification against high-resolution optical imagery (e.g., Sentinel-2 or Google Earth) is recommended before designing the field campaign to ensure sampling locations align with pure agricultural pixels.

The Topp et al. (1980) ε-mv conversion used in Eq. 3 was calibrated on mineral soils with clay contents generally below 40%. Marathwada vertisols can reach 60% clay, which may cause the Topp equation to underestimate mv. A soil-specific ε-mv calibration based on simultaneous dielectric measurements and gravimetric moisture sampling at Zadgaon is strongly recommended for the validation phase [18].

For the field validation campaign, measurements must be collected within ± 24 hours of Sentinel-1 acquisitions and must include: (i) volumetric soil moisture at 0-5 cm depth using calibrated TDR or gravimetric sampling; (ii) surface roughness profiling with a pin profiler across minimum 100 cm transects in at least two orthogonal directions per field, yielding both Hrms and correlation length; and (iii) direct dielectric constant measurements with a portable vector network analyzer. Land cover documentation crop type, canopy height, NDVI from co-registered Sentinel-2 is also needed to assess whether vegetation correction is required for each date.

For the October 2024 scene specifically, a Water Cloud Model correction using Sentinel-2 NDVI should be applied before MDM inversion, as kharif crop canopy is likely present and the bare-soil Dubois model will otherwise conflate vegetation and soil contributions. Extension to L-band SAR (ALOS-2 or, when operational data become available, the NISAR mission launched on July 30, 2025 and currently in commissioning) would provide deeper soil penetration and reduced vegetation attenuation, making it better suited to the kharif season. A comparative Dubois model assessment across C- and L-bands following MirMazloumi and Sahebi [9] would identify the optimal frequency for Parbhani vertisol conditions.

VII. CONCLUSION

This study has extracted and analyzed real Sentinel-1A VV backscatter values at Zadgaon, Parbhani district, Marathwada, for three acquisition dates in 2024, and applied the Dubois VV forward model to construct the solution manifold of plausible soil surface conditions at each date. The main findings are as follows.

Real σ⁰VV values of -10.44 dB (14 May), -10.22 dB (05 October), and −11.06 dB (10 November) was extracted from a 3×3-pixel window at the confirmed study coordinate (19.1676°N, 76.8317°E). The incidence angle was effectively constant across all three dates (38.045°-38.054°, $\Delta < 0.01°$), confirming that the observed σ⁰VV differences are attributable to changes in soil surface conditions rather than acquisition geometry.

October 2024 records the highest backscatter, followed by May 2024 and then November 2024. The total seasonal range of 0.84 dB is narrower than typical for a bare agricultural field undergoing a full monsoon moisture cycle. This is interpreted as a result of the moisture-roughness compensation characteristic of

Marathwada vertisols: dry-season crack development raises roughness and partially sustains σ⁰VV despite low moisture, while post-monsoon crack closure reduces roughness and partially offsets the moisture-driven increase in σ⁰VV.

The Dubois VV solution manifold, derived analytically from each measured σ⁰VV, shows that the observations are consistent with a broad range of physically plausible soil surface states mv roughly 0.148–0.400 m³/m³ depending on assumed roughness. The solution manifold itself is a quantitative scientific result: it defines the retrieval envelope and identifies precisely what field measurements are needed to collapse it to a unique solution.

Soil health card data from KVK Parbhani (pH 7.92, EC 0.66 dS/m, OC 0.78%, available K 1109 kg/ha) confirm that Zadgaon is a representative Marathwada vertisol site with above-average organic carbon and clay-rich mineralogy consistent with the observed backscatter behavior. These data cannot validate the MDM retrieval outputs directly but provide a physically grounded context for their interpretation.

This study establishes the first site-specific Sentinel-1 σ⁰VV dataset and Dubois VV solution manifold for a Parbhani district study location, along with a fully documented, reproducible SNAP preprocessing protocol. It lays the foundation for a field-validated soil surface parameter retrieval study at the same site, which will require synchronized measurements of mv, s, and ε timed to coincide with future Sentinel-1 acquisitions.

REFERENCES

[1] Costantini, E.A.C., Castaldini, M., Diago, M.P., et al. (2018). Effects of soil erosion on agro-ecosystem services and soil functions: A research agenda. Catena, 163, 19–27. https://doi.org/10.1016/j.catena.2017.11.025

[2] Petropoulos, G.P., et al. (2015). Surface soil moisture retrievals from remote sensing: Current status, products & future trends. Physics and Chemistry of the Earth, 83, 36–56. https://doi.org/10.1016/j.pce.2015.02.009

[3] Zeng, J., et al. (2023). Microwave Remote Sensing of Soil Moisture. Remote Sensing, 15(17), 4243. https://doi.org/10.3390/rs15174243

[4] Solanke, D., Yadav, B., Sawant, S., & Sayyad, S. (2025). SAR Remote Sensing of Soil: An Exploration of Surface Parameters Using Microwave Technology in the Semi-Arid Marathwada Region, India. International Research Journal of Natural and Applied Sciences, 12(10), 44–56.

[5] Solanke, D., Yadav, B., Sawant, S., & Sayyad, S. (2024). Unveiling Soil Characteristics: The Role of Microwave SAR in Surface Moisture Parameter Analysis. Technical Report, Shri Chhatrapati Shivaji College, Omerga.

[6] Haokip, S.C., et al. (2025). Approaches for Assessment of Soil Moisture with Conventional Methods, Remote Sensing, UAV, and Machine Learning Methods — A Review. Water, 17(16). https://doi.org/10.3390/w17162388

[7] Das, K., et al. (2015). Present status of soil moisture estimation by microwave remote sensing. Cogent Geoscience, 1(1). https://doi.org/10.1080/23312041.2015.1084669

[8] Shang, J., et al. (2022). Recent advancement of synthetic aperture radar systems and their applications to crop growth monitoring. InTechOpen. https://doi.org/10.5772/intechopen.102917

[9] MirMazloumi, S.M., & Sahebi, M.R. (2016). Assessment of different backscattering models for bare soil surface parameters estimation from SAR data in band C, L and P. European Journal of Remote Sensing, 49(1), 261–278. https://doi.org/10.5721/EuJRS20164914

[10] Torres, R., et al. (2012). GMES Sentinel-1 mission. Remote Sensing of Environment, 120, 9–24. https://doi.org/10.1016/j.rse.2011.05.028

[11] Baghdadi, N., et al. (2016). A new empirical model for radar scattering from bare soil surfaces. Remote Sensing, 8(11), 920. https://doi.org/10.3390/rs8110920

[12] Mirsoleimani, H.R., Sahebi, M.R., Baghdadi, N., & El Hajj, M. (2019). Bare Soil Surface Moisture Retrieval from Sentinel-1 SAR Data Based on the Calibrated IEM and Dubois Models Using Neural Networks. Sensors, 19(14), 3209. https://doi.org/10.3390/s19143209

[13] Brunelli, B., De Giglio, M., Magnani, E., & Dubbini, M. (2024). Surface soil moisture estimate from Sentinel-1 and Sentinel-2 data in agricultural fields in areas of high vulnerability to climate variations: the Marche region (Italy) case study. Environment, Development and

Sustainability, 26, 24083–24105. https://doi.org/10.1007/s10668-023-03635-w

[14] Dubois, P.C., van Zyl, J., & Engman, T. (1995). Measuring soil moisture with imaging radars. IEEE Transactions on Geoscience and Remote Sensing, 33(4), 915–926. https://doi.org/10.1109/36.406677

[15] Sahebi, M.R., & Angles, J. (2010). An inversion method based on multi-angular approaches for estimating bare soil surface parameters from RADARSAT-1. Hydrology and Earth System Sciences, 14(11), 2355–2366. https://doi.org/10.5194/hess-14-2355-2010

[16] Ghorbanian, A., Sahebi, M.R., & Mohammadzadeh, A. (2019). Optimization approach to retrieve soil surface parameters from single-acquisition single-configuration SAR data. Comptes Rendus Geoscience, 351(1), 69–80. https://doi.org/10.1016/j.crte.2018.09.003

[17] Topp, G.C., Davis, J.L., & Annan, A.P. (1980). Electromagnetic determination of soil water content: Measurements in coaxial transmission lines. Water Resources Research, 16(3), 574–582. https://doi.org/10.1029/WR016i003p00574

[18] Dirksen, C., & Dasberg, S. (1993). Improved calibration of Time Domain Reflectometry soil water content measurements. Soil Science Society of America Journal, 57(3), 660–667. https://doi.org/10.2136/sssaj1993.03615995005700030005x

[19] Rao, S.S., et al. (2013). Modified Dubois Model for Estimating Soil Moisture with Dual Polarized SAR Data. Journal of the Indian Society of Remote Sensing, 41(4), 865–872. https://doi.org/10.1007/s12524-013-0274-3

[20] Burgi, P.M., Lohman, R.B., et al. (2021). High-Resolution Soil Moisture Evolution in Hyper-Arid Regions. Journal of Geophysical Research: Earth Surface, 126(12). https://doi.org/10.1029/2021JF006158